Li-Ion Batteries

International Edition: DOI: 10.1002/anie.201901938
German Edition: DOI: 10.1002/ange.201901938

Lithium Chlorides and Bromides as Promising Solid-State Chemistries for Fast Ion Conductors with Good Electrochemical Stability

Shuo Wang, Qiang Bai, Adelaide M. Nolan, Yunsheng Liu, Sheng Gong, Qiang Sun, and Yifei Mo**

Abstract: *Enabling all-solid-state Li-ion batteries requires solid electrolytes with high Li ionic conductivity and good electrochemical stability. Following recent experimental reports of Li_3YCl_6 and Li_3YBr_6 as promising new solid electrolytes, we used first principles computation to investigate the Li-ion diffusion, electrochemical stability, and interface stability of chloride and bromide materials and elucidated the origin of their high ionic conductivities and good electrochemical stabilities. Chloride and bromide chemistries intrinsically exhibit low migration energy barriers, wide electrochemical windows, and are not constrained to previous design principles for sulfide and oxide Li-ion conductors, allowing for much greater freedom in structure, chemistry, composition, and Li sublattice for developing fast Li-ion conductors. Our study highlights chloride and bromide chemistries as a promising new research direction for solid electrolytes with high ionic conductivity and good stability.*

All-solid-state lithium-ion batteries (ASBs) with inorganic lithium solid electrolytes (SEs) are regarded as promising next-generation energy storage devices. ASBs solve the safety issue caused by the flammability of organic liquid electrolyte and potentially provide higher energy density with Li metal anode and high-voltage cathode materials.[1] However, it has been a great challenge to develop solid-state Li-ion conductors with high Li^+ conductivity at room temperature comparable to that of liquid electrolytes and with good electrochemical stability for Li-ion batteries with a voltage of >4 V. Current research efforts on solid-state Li-ion conductors focus mostly on oxides and sulfides.[1a,b,2] Unfortunately, oxide and sulfide chemistries have an undesirable trade-off between ionic conductivity and stability. Sulfide-based solid-state Li-ion conductors such as $Li_{10}GeP_2S_{12}$ (LGPS) and $Li_7P_3S_{11}$ (LPS) show good ionic conductivity but narrow electrochemical windows and poor stability with electrodes, whereas oxide solid-state Li-ion conductors show significantly wider electrochemical windows but lower ionic conductivity.[3] These general trends in the electrochemical stability of oxides and sulfides have been confirmed by high-throughput calculations on a large number of materials.[1b,3c] According to the design principles for superionic conductors (SICs) established by computational studies[4] in sulfide SICs such as LGPS and LPS, Li ions migrate among face-sharing tetrahedral sites in a body-centered cubic (bcc) S-anion lattice. In SICs with non-bcc anion lattices such as garnet and NASICON oxides, the high conductivity is achieved by aliovalent doping to activate concerted migration of multiple Li ions, which has a low energy barrier.[5] Therefore, SICs often require a unique structural framework, a unique Li sublattice as produced by a highly doped composition, or both, which are difficult to achieve.[5] Alternative anion chemistries that can exhibit a low activation energy, good stability, and other desirable properties are a promising research direction for new SEs in ASBs.

In this study, using first principles computation, we demonstrate that chlorides and bromides are promising anion chemistries to simultaneously achieve high ionic conductivity, good stability, and many other desired attributes, and to overcome limitations of sulfide and oxide SEs. Halide materials for SEs have received modest research interest, with only a few materials reported as Li-ion conductors.[1e,6] Recently, Asano et al.[7] reported the new superionic conductor halides Li_3YCl_6 (LYC) and Li_3YBr_6 (LYB) exhibiting high ionic conductivity of approximately 1 mS/cm at room temperature and good electrochemical stability in addition to mechanical deformability, air stability, and easy synthesis and processing for large-scale fabrication. These new halide SEs were demonstrated in 4 V ASBs assembled with In-Li anode and $LiCoO_2$ (LCO) cathode with no coating layer.[7] LYC and LYB have outstanding properties and features distinct from known oxide- and sulfide-based SICs. Besides the different anion chemistry, LYC and LYB do not have highly doped compositions with Li stuffing and have anion sublattices with hexagonal close-packed (hcp) and face-centered cubic (fcc) structures, respectively, which are deemed to have much higher energy landscapes than the bcc anion lattice. A detailed study to understand why these new halide systems perform so well would shed light on the future materials design and development efforts of SICs.

In this work, we perform first principles calculations on LYC, LYB, and similar halides to reveal the diffusion mechanism and to quantify their electrochemical stability. In addition to detailed understanding of these new halide SEs,

[*] S. Wang, S. Gong, Q. Sun
Department of Materials Science and Engineering, College of Engineering, Peking University
Beijing 100871 (China)
E-mail: sunqiang@pku.edu.cn

S. Wang, Q. Bai, A. M. Nolan, Y. Liu, Y. Mo
Department of Materials Science and Engineering, University of Maryland
College Park, MD 20742 (USA)
E-mail: yfmo@umd.edu

Y. Mo
Maryland Energy Innovation, University of Maryland
College Park, MD 20742 (USA)

Supporting information and the ORCID identification number(s) for the author(s) of this article can be found under: https://doi.org/10.1002/anie.201901938.

our results confirmed that fast ion diffusion and good electrochemical stability are intrinsic to chloride and bromide anion chemistries, providing a new research direction of SEs for ASBs. LYC has an hcp anion sublattice with a space group of $P3m1$, while LYB has an fcc anion sublattice with a space group of $C2/m$. In both materials, the Y^{3+} cations and Li^+ ions occupy six-coordinated octahedral (Oct) sites with halogen anions. One third of six-coordinated cation sites are vacant with Li partial-occupancy disordering, providing a large number of sites for Li migration and thus a high carrier concentration needed for high ionic conductivity. To identify the atomic configurations with lowest energy for our calculations, we enumerated all symmetrically distinct configurations using electrostatic Ewald energy and density functional theory (DFT) calculations, following the procedure established in previous studies.[8] The DFT calculations in the study are performed using Vienna Ab initio Simulation Package (VASP)[9] within the projector augmented-wave (PAW) approach[10] using the Perdew–Burke–Ernzerhof (PBE) functional[11] under generalized gradient approximation (GGA). More details of computation methods are provided in the supporting information.

We performed ab initio molecular dynamics (AIMD) simulations to study Li^+ diffusion in the LYC and LYB, using the established scheme.[12] The AIMD simulations confirmed the fast Li ion diffusion in these two materials, consistent with experiments. In LYB, the extrapolated Li^+ conductivity σ_{RT} at 300 K is 2.2 mS/cm, in excellent agreement with the experimental value of 1.7 mS/cm, and the estimated activation energy E_a is 0.28 ± 0.02 eV, which is smaller than experimental barrier of 0.37 eV. For LYC, AIMD simulations predicted $\sigma_{RT} = 14$ mS/cm with a lower bound of 4.5 mS/cm, which is one to two orders of magnitude higher than the experimental reported value (0.51 mS/cm), and the calculated E_a of 0.19 ± 0.03 eV is also lower than the experimental value (0.40 eV). This discrepancy of ionic conductivity in LYC may be explained by its anisotropic conductive mechanism.

The different anionic frameworks of fcc LYB and hcp LYC result in different Li^+ diffusion mechanism and pathways, as shown in AIMD simulations (Figure 1 a–d). The actual Li^+ trajectory observed in AIMD simulations is consistent with the pathways obtained from the bond valence site energy method.[7] In fcc LYB, Li^+ diffusion occurs through a 3D isotropic network, and Li^+ ions hop to the other octahedral sites through tetrahedral (Tet) sites. In hcp LYC, the Li^+ diffusion is anisotropic with fast c-axis one-dimension (1D) diffusion channels, in which Li ions hop among adjacent face-sharing octahedral sites. These 1D c-channels are connected through ab-planes through tetrahedral interstitial sites with slower diffusivity forming an anisotropic 3D diffusion network (Figure 1 c,d). This diffusion anisotropy is confirmed by directional Li^+ diffusivity from AIMD simulations (Supporting Information, Figure S9).

Similar to $LiFePO_4$ (LFP),[13] the 1D diffusion channel in LYC is expected to be susceptible to channel-blocking defects, such as anti-site defect, impurity, and grain boundary, which may partially account for the discrepancy between experiments and AIMD results. The previous experiments by Asano et al.[7] reported significant disordering of Y and Li cations in

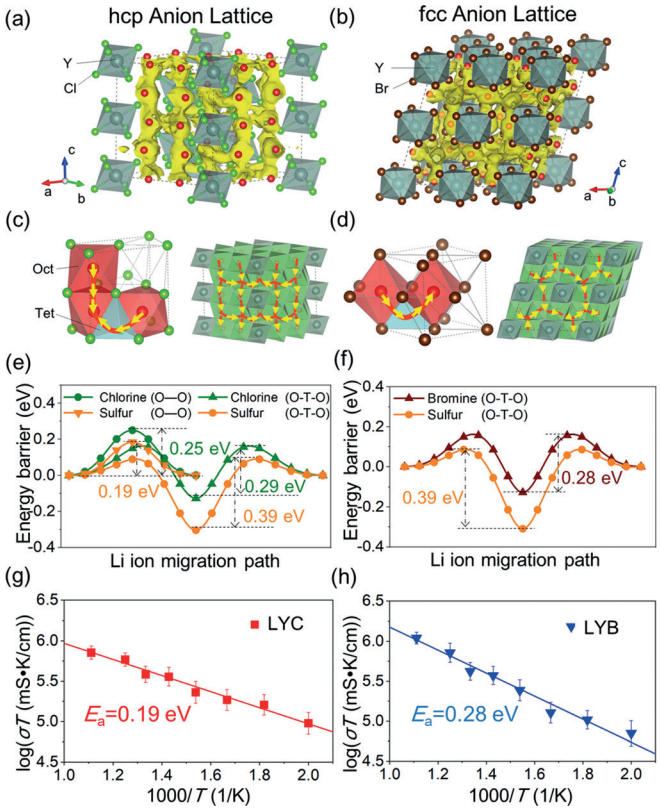

Figure 1. Crystal structures of a) LYC with hcp-like anion lattice and b) LYB with fcc-like anion lattice, superimposed with Li^+ probability density marked by yellow isosurfaces from AIMD simulations. The Li-ion migration pathways in c) LYC and d) LYB. The red and blue polyhedrons represent octahedral and tetrahedral interstitial sites, respectively. The energy landscape of single Li^+ migration in fixed e) hcp and f) fcc anion lattice at volume per anion of S^{2-} (LGPS: 40.0 Å^3), Cl^- (LYC: 37.4 Å^3) and Br^- (LYC:44.8 Å^3), respectively. Arrhenius plot of Li^+ diffusivity in g) LYC and h) LYB from AIMD simulations.

the materials. Our first principles calculations confirmed the low formation energy of 0.80 eV for exchanging Li and Y in the ordered lowest energy configuration of LYC (see the Supporting Information). This easy exchange of Y on Li ions is expected as Y and Li cations have similar local octahedral configurations and similar ionic radius, and may form during the synthesis and annealing of the materials. In our AIMD simulations on the structures with Y-on-Li anti-sites (Supporting Information, Figure S11, Table S2), the Li ionic conductivity at 300 K decreases by about an order of magnitude to 1.4–1.8 mS/cm (with a lower error bound of 0.3–0.4 mS/cm), and the activation energy increases to 0.31 ± 0.03 eV, which are in better agreement with the experimental values and support our proposed mechanism of channel-blocking defects. In addition, other effects such as impurity phases, grain boundaries, different microstructures, and local variations in composition resulting from different synthesis and processing conditions, may explain the discrepancy between experiments and computation.[1b]

Besides LYC and LYB, we found these close-packed hcp and fcc frameworks based on Cl and Br anion chemistry in general provide good ionic conductivity regardless of the

cation. Our first principles calculations predicted several isomorph structures substituting Y^{3+} in LYC and LYB with other 3^+ cations, such as Li_3MX_6 (M = Dy, Gd, Ho, La, Nd, Sc, Sm, Tb, Tm; X = Cl, Br), also have a good phase stability as measured by energy above the convex hull (ΔE_{hull}) (Supporting Information, Table S3).[1b,14] We selected Ho and Sc substituted compounds, which showed good phase stability with $\Delta E_{hull} < 30$ meV/atom, to further study their Li-ion diffusion (Supporting Information, Figure S10). These chlorides and bromides with other cations based on the same hcp and fcc anion framework, respectively, show high ionic conductivity of 10^{-4} to 10^{-3} S/cm (Table 1) comparable to well-known superionic conductors, such as LGPS and cubic-phase $Li_7La_3Zr_2O_{12}$.

Table 1: Calculated Li^+ conductivities and activation energies for different materials from AIMD simulations in comparisons of the experimental (Expt.) values at 300 K.

Composition	σ at 300 K [mS/cm]		Error bound $[\sigma_{min},\sigma_{max}]$ [mS/cm]	E_a [eV]	
	AIMD	Expt.		AIMD	Expt.
Li_3YCl_6	14	0.5	[4.5, 47]	0.19 ± 0.03	0.40
Li_3YBr_6	2.2	1.7	[0.7, 7.3]	0.28 ± 0.02	0.37
$Li_{10}GeP_2S_{12}$	14[11]	12[1a]	[8.1, 25]	0.21 ± 0.01[11]	0.23[1a]
$Li_7La_3Zr_2O_{12}$	1.1[11]	0.5[2a]	[0.5, 2.1]	0.26 ± 0.02[12]	0.30[2a]
Li_3ScCl_6	29	–	[8.2, 108]	0.18 ± 0.04	–
Li_3HoCl_6	21	–	[5.5, 84]	0.19 ± 0.03	–
Li_3ScBr_6	1.4	–	[0.2, 7.9]	0.30 ± 0.04	–
Li_3HoBr_6	3.8	–	[0.5, 27]	0.26 ± 0.04	–

In order to compare different anion chemistries, we modeled the energy landscape of single-Li^+ migration in fixed hcp and fcc anion sublattices of Cl, Br, and S with no M cations as a function of lattice volume, as in the study by Ceder et al.[4] (Supporting Information, Figure S4,S5). At the same lattice volume of LYC and LYB, hcp Cl and Br anion lattices have a low barrier of 0.25 eV for the Oct–Oct pathway along the *c*-channel and 0.29 eV for Oct–Tet–Oct pathway, and fcc Cl and Br anion lattices have a low barrier of 0.28 eV for the Oct–Tet–Oct pathway (Figure 1 e,f). These energy barriers agree with the activation energy obtained from AIMD simulations and experimental measurements. After considering the volume and site geometry of different anion chemistries, it can be found that fcc and hcp anion lattices of chlorides and bromides can exhibit an adequately low migration barrier of 0.2 to 0.3 eV, which is in general lower than those of approximately 0.4 eV in S-anion lattices in typical sulfides volume (Supporting Information, Figure S5 and S6). The energy barriers in close-packed structure of chlorides and bromides are low enough to achieve a high ionic conductivity of 10^{-3} S/cm if there is a decent level of carrier concentration. This low barrier for chlorides and bromides is intrinsic and a result of the monovalence of Cl and Br anions compared to the bivalence of O and S anions (see the Supporting Information). Compared to the S anion, the Cl anion has similar radius, higher electronegativity, and lower polarizability, which should not favor an easier Li-ion migration. The observed lower energy landscape of Cl anion lattice can be largely attributed to the lower valence of Cl^- compared to S^{2-}, because the weaker coulomb interactions with Li^+ lead to lower potential energy landscape. Other factors such as cations, Li concentrations, and the covalency of bonding may also affect the migration barrier.[6] In general, chlorides and bromides have low-barrier energy landscapes and are not limited to a specific anion sublattice, such as the bcc anion framework as sulfide SICs.

Because of this low energy landscape, chlorides and bromides do not require the activation of concerted migration of Li ions to achieve fast ion diffusion, as is necessary in oxide-based garnet and NASICON SICs. In our AIMD simulations of LYC and LYB, there is no notable concerted migration of multiple Li ions. The conductivity estimated from the self-diffusivity and Nernst–Einstein relation is close to the diffusivity estimated from the center of all mobile Li ions, which is in agreement with experimental conductivitly measurement. Since concerted migration requires significant Li stuffing in the host crystal structure, Cl and Br anion chemistries are not subject to these difficult structural requirements for oxide and sulfide SICs, and provide a broader range of structures, compositions, and Li sublattices for new fast ion-conducting SEs. Given there are fewer requirements for chlorides and bromides to have a low migration energy, the key design principle to achieve high ionic conductivity in these materials is to have a high level of carrier concentration, which is provided by a disordered Li sublattice in LYC and LYB.[6]

In addition to exceptional Li-ion conducting properties, our first principles computation also confirms wide electrochemical windows, poor electronic conductivity, and good interface compatibility with electrode, in these halide materials (see the Supporting Information). Our calculations based on Heyd–Scuseria–Ernzerhof functional[15] found that LYC and LYB have large band gaps of 6.02 eV and 5.05 eV (Figure 2 c,d), respectively, and are poor electronic conductors, which are crucial for SEs.[16] To obtain the thermodynamic intrinsic electrochemical windows for LYC and LYB, the equilibrium voltage profile and corresponding phase equilibria as a function of applied potential referenced to Li/Li^+ are calculated using the scheme[3b,c,17] based on the

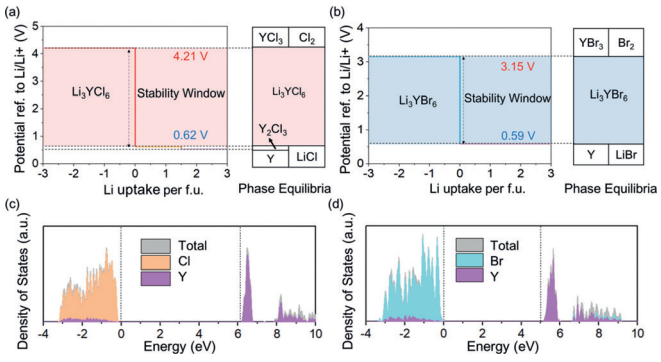

Figure 2. Calculated thermodynamic equilibrium voltage profile and phase equilibria of a) LYC and b) LYB. Calculated density of states (DOS) from HSE calculations for c) LYC and d) LYB.

Materials Project[18] (MP) database. Both LYB and LYC show wide electrochemical windows with anodic limits of 3.15 V and 4.21 V, respectively, and a cathodic limit of 0.59 and 0.62 V (Figure 2 a,b), respectively. These thermodynamic intrinsic windows are significantly wider than many current sulfide and oxide SEs such as LGPS (1.72–2.29 V), Li_3PS_4 (1.71–2.31 V), LISICON (1.44–3.39 V), and $Li_{0.33}La_{0.56}TiO_3$ (1.75–3.71 V).[3b,d] While their reduction limits are lower than that of many other SEs, LYC, and LYB are still not thermodynamically stable with Li metal, and are calculated to have a small decomposition energy of 0.18 and 0.19 eV/atom, respectively, in equilibrium with Li metal. This may explain the In–Li anode with a Li/Li^+ potential of 0.6 V used in the ASB cells demonstrated by Asano et al.[7] The high oxidation stability of LYC at >4 V supports its use for current high-potential cathode materials in Li-ion batteries, and is consistent with the reported good electrochemical performance of ASB cells using LCO cathode mixed with LYC SEs without protective coating layers. The slightly inferior oxidation stability of LYB at <4 V is inadequate for the full range of cathode stability, which may explain why Asano et al. did not use LYB as an ion-conducting mixture with LCO cathode.[7]

The high oxidation stability is an intrinsic property of the chloride and bromide anion chemistries. This general trend of electrochemical windows and anion chemistries is confirmed in our calculations with Li–M–X ternary compounds (M = cation, X = F, Cl, Br, I, O, S) in Figure 3 and Table S5 in the

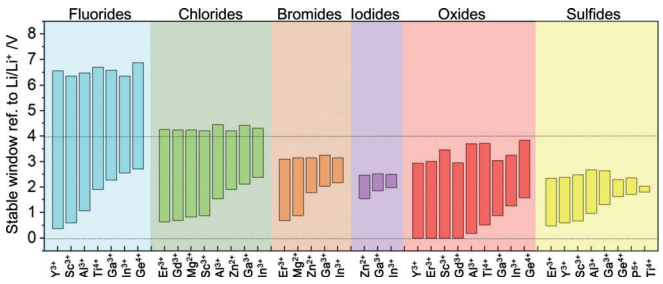

Figure 3. Calculated thermodynamics intrinsic electrochemical windows of Li–M–X ternary fluorides, chlorides, bromides, iodides, oxides, and sulfides. M is a metal cation at its highest common valence state.

Supporting Information. While fluorides have the best oxidation stability, chlorides strike a balance between reduction and oxidation stability. On the cathode side, chlorides have a significant advantage in stability over oxides and sulfides, and adequately satisfy the 4 V potential of current Li-ion battery cathodes. In general, chlorides and bromides exhibit wide electrochemical windows and large band gaps, as promising chemistries for SEs to replace sulfides and oxides.

The interface compatibility with electrode materials is also critical for ASB performance, such as coulombic efficiency (CE), interfacial resistance, and cycle life.[3] We investigated the possible interfacial reactions between LYC and LYB SEs and common cathode materials using the pseudo-binary model as in the previous study.[17] The reaction energy of LYC and LYB with LCO cathode is as small as <45 meV/atom, which is comparable to oxide SEs and is one order of magnitude less than sulfides.[17] LYC remains stable with delithiated $Li_{0.5}CoO_2$, with an even smaller reaction energy of 24 meV/atom, suggesting good stability during voltage cycling. This calculated good interface stability of LYC with LCO are consistent with the high CE (94.8%) in the initial cycle of the ASB cell with mixed LYC and LCO cathode without a protective coating.[7] In comparison, most sulfide SEs suffer favorable decomposition with delithiated cathodes at charged state,[17] and ASBs with lithium thiophosphate SEs showed an initial cycle CE of 84.0%.[7] This good compatibility with LCO is also confirmed for other common cathode materials, such as $LiFePO_4$ (Supporting Information, Table S6). This good stability of lithium chlorides with delithiated cathode is a result of its good oxidation stability (see the Supporting Information). Therefore, lithium chloride compounds are generally promising SEs with good interfacial compatibility with the cathode.

In summary, we performed a first principles computation study on LYC and LYB SEs. The results of this study confirmed fast Li-ion conduction, wide electrochemical stability, and good cathode interface compatibility, consistent with experimental reports. As revealed by AIMD simulations, the Li^+ diffusion mechanism in both LYC and LYB in close-packed hcp and fcc anion lattice is Li-ion hopping among octahedral sites through existing vacant sites with a low barrier. The fcc LYB shows isotropic fast Li^+ diffusion, and hcp LYC shows anisotropic diffusion with fast 1D *c*-channels, which may be susceptible to blocking defects such as Y-Li anti-sites. The low migration energy barrier is intrinsic for Cl and Br anion sublattices, thanks to the monovalence of Cl^- and Br^-. Thus, Cl and Br anion chemistries can achieve fast Li-ion conduction in a variety of anion sublattices, and do not require the rare bcc anion lattice as in current fast ion-conducting sulfides or the concerted migration mechanism in current fast ion-conducting oxides. Therefore, chlorides and bromides provide a much wider materials space for fast Li-ion conductors with fewer constraints on anion lattice and Li sublattice than current sulfide and oxide SICs. Furthermore, we found that chlorides and bromides generally exhibit wide electrochemical windows, poor electronic conductivity, and good cathode interface compatibility, and thus hold desirable conducting and stability properties for SE applications. In addition, these halide materials may also exhibit oxygen gas stability, easy synthesis and processing, and mechanical deformability, which are also required for good performance and large-scale fabrication of ASBs. Thus, chlorides and bromides are highly promising alternative chemistries for SEs in ASBs.

Acknowledgements

S.W. acknowledges the financial support from China Scholarship Council. Q.S. acknowledges the grant support from the National Key Research and Development Program of China (2016YFB0100200), and from the National Natural Science Foundation of China (21773003 and 21573008). Y.M. acknowledges the support from National Science Foundation

under award No. 1550423. This research used computational facilities from the University of Maryland supercomputing resources and the Maryland Advanced Research Computing Center (MARCC).

Conflict of interest

The authors declare no conflict of interest.

Keywords: all-solid-state batteries · first principles computation · halides · Li-ion batteries · solid electrolytes

How to cite: *Angew. Chem. Int. Ed.* **2019**, *58*, 8039–8043
Angew. Chem. **2019**, *131*, 8123–8127

[1] a) N. Kamaya, K. Homma, Y. Yamakawa, M. Hirayama, R. Kanno, M. Yonemura, T. Kamiyama, Y. Kato, S. Hama, K. Kawamoto, A. Mitsui, *Nat. Mater.* **2011**, *10*, 682–686; b) A. M. Nolan, Y. Zhu, X. He, Q. Bai, Y. Mo, *Joule* **2018**, *2*, 2016–2046; c) J. Janek, W. G. Zeier, *Nat. Energy* **2016**, *1*, 16141–16144; d) J. Li, C. Ma, M. Chi, C. Liang, N. J. Dudney, *Adv. Energy Mater.* **2015**, *5*, 1401408; e) J. C. Bachman, S. Muy, A. Grimaud, H.-H. Chang, N. Pour, S. F. Lux, O. Paschos, F. Maglia, S. Lupart, P. Lamp, L. Giordano, Y. Shao-Horn, *Chem. Rev.* **2016**, *116*, 140–162.

[2] a) R. Murugan, V. Thangadurai, W. Weppner, *Angew. Chem. Int. Ed.* **2007**, *46*, 7778–7781; *Angew. Chem.* **2007**, *119*, 7925–7928; b) H. Yamane, M. Shibata, Y. Shimane, T. Junke, Y. Seino, S. Adams, K. Minami, A. Hayashi, M. Tatsumisago, *Solid State Ionics* **2007**, *178*, 1163–1167; c) R. Kanno, M. Murayama, *J. Electrochem. Soc.* **2001**, *148*, A742–A746; d) V. Thangadurai, S. Narayanan, D. Pinzaru, *Chem. Soc. Rev.* **2014**, *43*, 4714–4727; e) Z. Zhang, Y. Shao, B. Lotsch, Y.-S. Hu, H. Li, J. Rgen Janek, L. F. Nazar, C.-W. Nan, J. Maier, M. Armand, L. Chen, *Energy Environ. Sci.* **2018**, *11*, 1945–1976; f) K. H. Park, Q. Bai, D. H. Kim, D. Y. Oh, Y. Zhu, Y. Mo, Y. S. Jung, *Adv. Energy Mater.* **2018**, *8*, 1800035.

[3] a) F. Han, Y. Zhu, X. He, Y. Mo, C. Wang, *Adv. Energy Mater.* **2016**, *6*, 1501590; b) Y. Zhu, X. He, Y. Mo, *ACS Appl. Mater. Interfaces* **2015**, *7*, 23685–23693; c) Y. Zhu, X. He, Y. Mo, *Adv. Sci.* **2017**, *4*, 1600517; d) W. D. Richards, L. J. Miara, Y. Wang, J. C. Kim, G. Ceder, *Chem. Mater.* **2016**, *28*, 266–273.

[4] Y. Wang, W. D. Richards, S. P. Ong, L. J. Miara, J. C. Kim, Y. Mo, G. Ceder, *Nat. Mater.* **2015**, *14*, 1026–1031.

[5] X. He, Y. Zhu, Y. Mo, *Nat. Commun.* **2017**, *8*, 15893.

[6] N. Adelstein, B. C. Wood, *Chem. Mater.* **2016**, *28*, 7218–7231.

[7] T. Asano, A. Sakai, S. Ouchi, M. Sakaida, A. Miyazaki, S. Hasegawa, *Adv. Mater.* **2018**, *30*, 1803075.

[8] a) Y. Mo, S. P. Ong, G. Ceder, *Chem. Mater.* **2012**, *24*, 15–17; b) X. He, Y. Mo, *Phys. Chem. Chem. Phys.* **2015**, *17*, 18035–18044.

[9] G. Kresse, J. Furthmüller, *Phys. Rev. B* **1996**, *54*, 11169.

[10] P. E. Blöchl, *Phys. Rev. B* **1994**, *50*, 1795.

[11] J. P. Perdew, K. Burke, M. Ernzerhof, *Phys. Rev. Lett.* **1996**, *77*, 3865.

[12] X. He, Y. Zhu, A. Epstein, Y. Mo, *npj Comput. Mater.* **2018**, *4*, 18.

[13] R. Malik, D. Burch, M. Bazant, G. Ceder, *Nano Lett.* **2010**, *10*, 4123–4127.

[14] S. P. Ong, L. Wang, B. Kang, G. Ceder, *Chem. Mater.* **2008**, *20*, 1798–1807.

[15] J. Heyd, G. E. Scuseria, *J. Chem. Phys.* **2004**, *121*, 1187–1192.

[16] F. Han, A. S. Westover, J. Yue, X. Fan, F. Wang, M. Chi, D. N. Leonard, N. J. Dudney, H. Wang, C. Wang, *Nat. Energy* **2019**, *4*, 187–196.

[17] Y. Zhu, X. He, Y. Mo, *J. Mater. Chem. A* **2016**, *4*, 3253–3266.

[18] A. Jain, S. P. Ong, G. Hautier, W. Chen, W. D. Richards, S. Dacek, S. Cholia, D. Gunter, D. Skinner, G. Ceder, *APL Mater.* **2013**, *1*, 011002.

Manuscript received: February 13, 2019
Revised manuscript received: March 25, 2019
Accepted manuscript online: April 11, 2019
Version of record online: May 15, 2019

